Dalton Transactions

Accepted Manuscript

ROYAL SOCIETY OF CHEMISTRY

www.rsc.org/dalton

Journal Name

RSCPublishing

ARTICLE

A Highly Stable Indium Phosphonocarboxylate Framework as Multifunctional Sensor for Cu^{2+} and Methylviologen Ions

Wenyan Dan, Xiaofeng Liu, Mingli Deng, Yun Ling, Zhenxia Chen* and Yaming Zhou*

Cite this: DOI: 10.1039/x0xx00000x

Received 00th January 2012,
Accepted 00th January 2012

DOI: 10.1039/x0xx00000x

www.rsc.org/

An indium phosphonocarboxylate framework, $\{H_3O[In(pbpdc)]\cdot 3H_2O\}_n$ (**InPCF-1**) (pbpdc=4'-phosphonobiphenyl-3,5-dicarboxylate) was hydrothermally synthesized. The structure of **InPCF-1** features the inorganic chains as rod-shaped second building units. The rod-packing arrangement results in a three-dimensional (3-D) framework with novel (3,4,5)-connected net. Studies of the gas adsorption, thermal and chemical stability of **InPCF-1** demonstrated its adsorption capacity for CO_2, selective separation of CO_2 over O_2 and N_2, high thermal stability, remarkable chemical resistance to boiling water, ethyl alcohol, and methylbenzene. Importantly, **InPCF-1** shows selective and sensitive response to Cu^{2+} ion. It also serves as a sensor for methylviologen.

Introduction

Metal phosphonate frameworks, which have advantages in thermal and chemical stabilities for industrial applications,[1,2] are a class of promising materials with great potentials of catalysis,[3] gas storage/separation,[4] magnetism,[5] and proton conduction.[6] Recently, many research interests are focused on the luminescent sensing materials for Cu^{2+} and small organic molecules known as environmental pollutants.[7] Although various luminescent metal-organic frameworks (MOFs) based on chromophoric linkers and metal centers (mostly lanthanide ions) have already been reported,[8] metal phosphonates were rarely used for sensing application. Their preference to form condensed structures has limited their sensing functions to metal ions and organic molecules. On the other hand, the free Lewis basic sites within the porous luminescent frameworks are very important for immobilizing Cu^{2+} ions.[9] Phosphonates do not form the types of secondary building units with metal ions as the carboxylates do, so rational design of the target structures is nearly impossible. To date, there has been minimal focus on the metal phosphonate frameworks with functional sites. Thus, the exploration and synthesis of chemical stable metal phosphonate frameworks for selective and sensitive luminescent sensors are in high demand but challenging.

Among the various metal phosphonate frameworks, most of them were constructed by phosphonate ligands and divalent transition metal.[10] Few trivalent metals like Al^{3+}, In^{3+}, and Ga^{3+} phosphonate frameworks were reported in spite of a large number of trivalent metal carboxylates.[11] As we know, In^{3+} exhibits excellent structural and coordinative flexibility such as InO_6 octahedra, InO_7 pentagonal bi-pyramids, and InO_8 dodecahedra, resulting in all kinds of fascinating structures and unique applications for gas storage, catalysis, and luminescent substrate.[12] Herein, we used a lab-made phosphonocarboxylate ligand, 4'-phosphonobiphenyl-3,5-dicarboxylic acid (H_4pbpdc) and In^{3+} to build novel metal-phosphonate frameworks. This ligand was designed based on the following reasons: (i) In^{3+} is able to coordinate with the phosphonate group to form stable inorganic cluster or chain and the elongated biphenyl part of H_4pbpdc will help to generate highly porous framework; (ii) the multifunctional groups of carboxylate and phosphonate have the possibility to remain uncoordinated and act as sites to recognize small organic molecules and metal ions. An indium phosphonocarboxylate framework, $\{H_3O[In(pbpdc)]\cdot 3H_2O\}_n$ (**InPCF-1**) was hydrothermally synthesized. The structure has an inifinite inorganic chain as second building unit. The rod-packing arrangement of these chains results in a 3-D framework with open 1-D channels. The porosity has been confirmed by CO_2 adsorption. As far as we know, it is the first indium phosphonate open-framwork. **InPCF-1** shows high thermal stability and excellent chemical stability in various solvents. Luminescent measurements for **InPCF-1** reveal sensitive response for Cu^{2+} and methylviologen ions.

Experimental

Materials and methods

All reagents for syntheses were purchased from commercial sources and used as received except dimethyl-5-boronic acid pinacol ester-isophtalate and 4'-phosphonobiphenyl-3,5-dicarboxylic acid, which were prepared according to literatures.[13,14] Thermogravimetric (TGA) analyses were carried out on a METTLER TOLEPO TGA/SDTA851 analyzer in the temperature range of 30 ~ 800 °C under N_2 flow with a heating rate of 10 °C min^{-1}. Elemental analyses (C, H) were performed on an Elementar Vario EL III microanalyzer. IR spectra were recorded from a KBr pellets on a Nicolet Nexus 470 FT-IR spectrometer in the range of 4000 ~ 400 cm^{-1}. Powder X-ray diffraction (PXRD) patterns were measured using a Bruker Advance D8 powder diffractometer at 40 kV, 40 mA for Cu Kα radiation (λ = 1.5406 Å), with a scan speed of 0.2 s/step and a step size of 0.05 ° (2θ). Varied-temperature PXRD patterns were obtained after the sample was heated under air from 60 °C to 400 °C and kept for 1 hour at different temperature. Energy dispersive X-ray spectroscopy (EDS) data were obtained on a Philips XL-30 scanning electron microscope. A Micromeritics ASAP 2020 surface area analyzer was used to measure gas adsorption. The sorption isotherms for methanol, ethanol and water were measured with an automatic gravimetric adsorption apparatus (IGA-003 series, Hiden Isochema Ltd.) at 298 K. Before measurement, the activated sample (**InPCF-1a** with the composition of $[In(Hpbpdc)]_n$) were prepared by immersing as-made sample in CH_3OH for three days and subsequently heating at 180 °C in a quartz tube under high vacuum for 12 h.

Photoluminescence spectra were recorded on a Cary Eclipse EL00063372 spectrofluorometer. The scanning speed was performed at the speed of 600 nm·min^{-1}, the slit width of excitation and emission is 10 nm. For the experiment of sensing metal and methylviologen ions, the activated **InPCF-1** emulsions were prepared by introducing 0.5 mg of **InPCF-1a** powder into 4.00 mL DMF and sonicating for 10 minutes.

Synthesis of $\{H_3O[In(pbpdc)]\cdot 3H_2O\}_n$ (InPCF-1)

$In(NO_3)_3\cdot 6H_2O$ (0.1 mmol, 0.040 g) and H_4pbpdc (0.1 mmol, 0.032g) were dissolved in H_2O (10 mL) and 0.05 mL of 30 wt% HF was added. The mixture was stirred at room temperature for 2 h, and then transferred into a 15 mL Teflon-lined stainless steel autoclave. Then the mixture was heated at 180 °C for 5 days, followed by cooling to room temperature at a rate of 10 °C/min. Colorless rod crystals were collected by filtration (yield: 48% based on H_4pbpdc). Anal. calcd for $\{H_3O[In(pbpdc)]\cdot 3H_2O\}_n$ (506.07): C, 33.23; H, 3.19; Found: C, 34.52; H, 2.95. IR (KBr, cm^{-1}): 3434(m), 1614(m), 1565(m), 1448(m), 1400(w), 1383(w), 1368(w), 1156(w), 1130(w), 1057(m), 1376(m), 1137(m), 1065(m), 1025(w), 996(w), 776(m), 751(m), 704(m), 602(m).

X-ray crystal structure determination

Single-crystal X-ray diffraction measurements were carried out on a Bruker Apex Duo diffractometer with graphite monochromated Mo-Kα radiation (λ = 0.71073 Å) at 293 K. Data reduction was performed with the SAINT and empirical absorption corrections were applied by the SADABS program. The structure was solved by direct methods using the SHELXS program and refined with SHELXL program.[15] Heavy atoms and other non-hydrogen atoms are directly obtained from different Fourier maps. Final refinements were performed by the full-matrix least-square method with anisotropic thermal parameters for all non-hydrogen atoms on F^2. The hydrogen atoms on carbon atoms were added theoretically and not refined. The lattice water molecules are highly disordered and thus show poor thermal parameters. The hydrogen atoms on water are missing from the refinement models. The composition of **InPCF-1** was given as $\{H_3O[In(pbpdc)]\cdot 3H_2O\}_n$ by combining crystallography and TGA results, with only three lattice water molecules were determined by single crystal X-ray diffraction. Crystallographic data are listed in Table 1, and selected bond length and angles are listed in Table S1†.

Table 1 Crystal data and structure refinement for **InPCF-1**.

Entry	**InPCF-1**
Empirical formula	$C_{14}H_{14}InO_{10}P$
Formula weight	488.05
Crystal system	Tetragonal
space group	*P*4/*mnc*
a/Å	23.474(3)
c/Å	6.6926(9)
α/°	90
V/Å^3	3687.9(8)
Z	8
ρ_{calcd}/ g·cm^{-3}	1.733
μ /mm^{-1}	1.417
F(000)	1880
h k l range	$-27\le h\le 25$, $-27\le k\le 27$, $-7\le l\le 7$
θ range/ °	1.23 to 25.01
Collected / Unique	21607 / 1778
Data/restraints/parameters	1778 / 0 / 157
R_{int}	0.1108
GOF on F^2	1.174
R_1 and ωR_2[$I > 2\sigma(I)$]	$R_1 = 0.0462$ $\omega R_2 = 0.1175$
R_1 and ωR_2[all data]	$R_1 = 0.0720$ $\omega R_2 = 0.1432$
$\Delta\rho$max, $\Delta\rho$min/ e·Å^{-3}	1.075, -0.692

[a] $R_1 = \Sigma||F_o| - |F_c||/\Sigma|F_o|$. [b] $wR_2 = [\Sigma w(F_o^2 - F_c^2)^2/\Sigma w(F_o^2)^2]^{1/2}$

Results and discussion

Structural description

Single-crystal X-ray diffraction measurement reveals that **InPCF-1** crystallizes in the tetragonal space group of *P*4/*mnc*. The In^{3+} ion and $pbpdc^{4-}$ ligand with occupation of 0.5 are located on the (001) plane. There are one and a half guest water molecules in the asymmetric unit. As shown in Fig. 1a, In^{3+} ion is hexa-coordinated and resides in the center of a distorted octahedron defined by three phosphonate oxygens and three carboxylate oxygens with the In-O bonds ranging from 2.071(6) Å to 2.303(7) Å. P atom resides in the

center of a distorted tetrahedron. The P-O bond distances are close from 1.528(5) Å to 1.529(7) Å and bond length of C-P bond is 1.822(10) Å. The distances of four C-O bonds on two carboxylate groups range from 1.246(14) to 1.261(12) Å. All the phosphonate and carboxylate groups are considered as deprotonated according to the short bond distances and the charge balance proton is attached on the lattice water molecule. Each $pbpdc^{4-}$ bonds to five indium ions through three phosphonate oxgen atoms and two carboxylate groups, one of which coordinates with indium ion in a bidentate mode and the other in a monodentate mode. The phosphonate group adopts a [3.111] coordination mode using the Harris notation.[16]

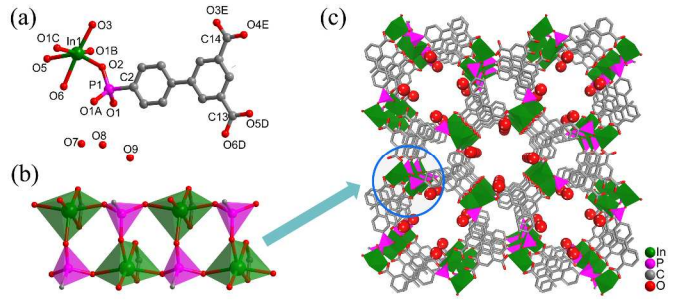

Fig. 1 (a) The structural unit of **InPCF-1**. Symmetry codes: A: x, y, 2-z; B: 0.5-y, 0.5-x, 1.5-z; C: 0.5-y, 0.5-x, 0.5+z; D: y, 1-x, z; E: -x, 1-y, z. (b) Ladder-like chain composed of InO_6 octahedron and O_3PC tetrahedron in the title complexes. (c) Packing of **InPCF-1** as viewed slightly off the *c* axis. The water molecules were omitted for clarity and the uncoordinated carbonyl oxygens were highlighted.

The InO_6 octahedra and O_3PC tetrahedra were alternately corner-shared to form an infinite ladder-like chain along *c* axis as shown in Fig. 1b. This kind of ladder chain have been previously reported in some indium phosphates,[17] which suggest the correlation between phosphonate open-frameworks and inorganic metal phosphates. The ladder-like chains can be considered as $[In(PO_3)(CO_2)_2]_\infty$ rod second building units (SBUs) as those defined in the metal carboxylates.[18] The biphenyl part of H_4pbpdc ligands linked each rod SBU to four neighboring SBUs in the *a* and *b* directions, resulting in a one dimensional (1-D) channel with the size of 7.19 × 7.19 Å by considering the Van der Waals radius (Fig. 1c and S1, ESI†). The lattice water molecules were located in the straight channels and interacts with framework by hydrogen bonds with the O···O (D···A) distances of 2.78(3) and 2.991(18) Å (Table S2†). The void volume occupied by the neutral and protonated lattice water molecules is 1172.0 $Å^3$ (31.8 %) as estimated by PLATON using a probe of 1.2 Å.[19]

To better understand the structure of **InPCF-1**, the topology was analyzed in detail using the TOPOS program.[20] Considering the $-CPO_3$ group as a 4-connected node, the dicarboxyl-biphenyl linker as a 3-connected node and In^{3+} as a 5-connected node, the total 3-D network exhibits a trinodal (3,4,5)-connected topology with point symbol of $(4^2{\cdot}6^4{\cdot}7^3{\cdot}8)(4^2{\cdot}6^4)(6{\cdot}7^2)$ (Fig. 2). According to the search results from reticular Chemistry Structure Resource Database and other literatures, there are only six trinodal (3,4,5)-connected nets, including the symbol name of **csp**, **hms-a**, **sqs-a**, **tff**, [21a] and the other two with point symbol of $(6^3)(4^2{\cdot}8^4)(4{\cdot}6^3{\cdot}8^6)$[21b] and $(7{\cdot}8^2)(4^2{\cdot}6^2{\cdot}7^2)(4^2{\cdot}6{\cdot}7^3{\cdot}8^2{\cdot}9^2)$.[21c] **InPCF-1** exhibits a completely new topology in MOF chemistry.

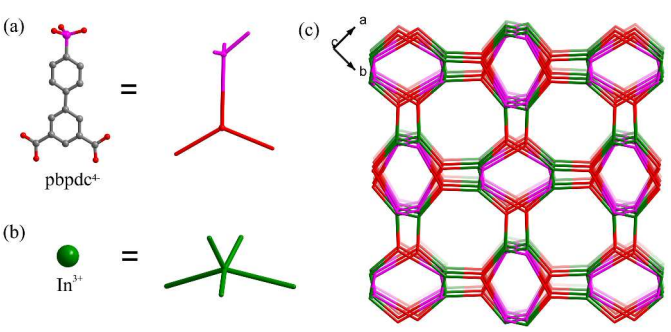

Fig. 2 Topology of **InPCF-1**: (a) the simplified $pbpdc^{4-}$ in a 3,4-connected node; (b) the simplified In in a 5-connected node; (c) the 3-nodal net of **InPCF-1**.

Thermal and chemical stability

Thermogravimetric analysis (Fig. S2†) and Varied-temperature PXRD (Fig. 3) were performed to testify the thermal stability of **InPCF-1**. **InPCF-1** shows three distinct steps of approximately 56.3 % weight losses. The first weight loss of about 14.1 % before 140 °C was attributed to the removal of four water molecules (calc. 14.2 %). Then it loses weight in two continuous steps after a short platform. One weight loss between 250 and 350 °C was attributed to partial framework decomposition. The sharp weight loss after 350 °C corresponded to the departure of the organic ligands and collapse of framework. The residue is considered as mixture of $InPO_3$ and In_2O_3 Varied-temperature PXRD patterns obtained at increasing temperatures show the peak intensities decrease after 250 °C due to partial framework decomposition. The framework collapses after 400 °C.

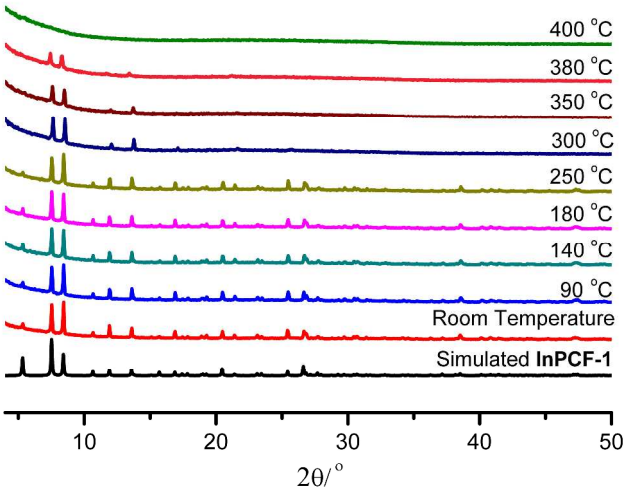

Fig. 3 PXRD patterns of **InPCF-1** in air from room temperature to 400 °C.

The chemical stability of **InPCF-1** was examined by suspending sample in boiling water ethanol, and toluene, conditions that reflect extreme operational parameters of typical chemical processes. PXRD patters collected for the samples being soaked in boiling water, ethanol, and toluene for 1~7 days showed **InPCF-1** maintained its structure (Fig. S3† and S4†). It can be concluded that **InPCF-1** has excellent chemical stability as well as high thermal stability. The high stability of **InPCF-1** might be

attributed to strong coordination bonds between metal and phosphonate oxygen. In addition, the high coordination number of indium, the rigid ladder-like inorganic chains, and the close packing between the aromatic ligand were beneficial for improving the stability of **InPCF-1**.

Adsorption properties

Adsorption experiments were then carried out to confirm the porosity. The activated sample of **InPCF-1** shows no significant adsorption for N_2 at 77 K. Given that the framework has channels larger than N_2 molecules, it seemed that some surface defects block access to the channels, which frequently happens in structures with 1-D pores.[22] In the case of CO_2, which has a large quadrupole moment, it can diffuse through the barrier. The adsorption at 298 K gave a typical Type I isotherm (Fig. 4a and Fig. S5†). The adsorption and desorption are almost reversible. The total uptake was 21 $cm^3(STP)\cdot g^{-1}$ under 800 mmHg. Adsorption capacity increases to 32 $cm^3(STP)\cdot g^{-1}$ with the decrease of the temperature at 273 K. The BET surface area is calculated to be 246 $m^2\cdot g^{-1}$ (Langmuir surface area, 269 $m^2\cdot g^{-1}$) according to the data at 273 K. The pore volume is calculated to be 0.068 cm^3/g using the maximum measured CO_2 capacity of 32 $cm^3(STP)$ g^{-1} and a CO_2 density of 0.925 g/cm^3 in the liquid state. Given accessible solvent void space of 375.3 $Å^3$ per unit cell by using a probe sphere of 1.6 Å equal to the kinetic radius of CO_2, the pore volume calculated from the dehydrated crystal structure by Material Studio is 0.065 cm^3/g. The isotherms were fitted to the Virial model and the isosteric heat of CO_2 adsorption is calculated (Fig. S6† and S7†). At zero coverage, indicating CO_2 interaction with the most energetically favored sites, the enthalpy is 33.9 $kJ\cdot mol^{-1}$, which is significantly higher than the enthalpy of liquefaction of CO_2 (17 $kJ\cdot mol^{-1}$). The high Q_{st} value in **InPCF-1** might be due to the interactions between the carbonyl groups and CO_2.[23] The N_2 and O_2 adsorption results indicate that the framework of **InPCF-1** shown nil adsorption at room temperature and the uptake amount is ca. 3.15 and 0.70 cm^3/g at a pressure of 800 mmHg, respectively. In the case of post combustion CO_2 capture, the partial pressures of CO_2, N_2, and O_2 are 0.15, 0.75, and 0.03 bar,[24] respectively. The selectivity of CO_2 over N_2 and O_2, based on the single-component adsorption results, was simply calculated using the reported equation.[25] The selectivity of CO_2 over N_2 is 22, and the selectivity of CO_2 over O_2 is 32; this suggests the potential selective adsorption of CO_2 over N_2 and O_2.

The porosity of **InPCF-1** was also confirmed by the liquid vapour adsorption at 298 K (Fig. 4b). The methanol adsorption isotherm of **InPCF-1** reveals a typical type-I curve for microporous materials. The maximum adsorption amount is 2.2 $mmol\cdot g^{-1}$ at P/P_0 = 0.94, which are equivalent to the adsorption of about 1.0 MeOH per formula unit. The water adsorbed amount (1.7 $mmol\cdot g^{-1}$, 0.8 H_2O per unit) is slightly lower than that of methanol. Ethanol adsorption measurement shows the isotherm similar to nonporous behavior, indicating that **InPCF-1** exhibits selectivity to sizes of the guests. All the isotherms show large hysteresis loops, which might due to the strong sorbent-sorbate interactions (Fig. S8†-S10†).

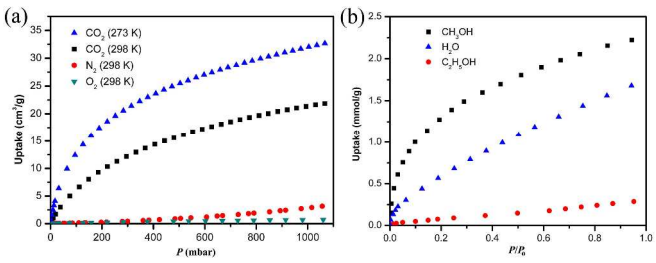

Fig. 4 (a) CO_2, N_2 and O_2 sorption isotherms of **InPCF-1a** measuring at 298 and 273 K. (b) Isotherms for the adsorption of methanol, ethanol, and water on **InPCF-1a** at 298 K.

Sensing of metal and organic ions

The solid luminescence of **InPCF-1a** and free ligand were investigated at room temperature under excitation at 290 nm (Fig. S11†). The free H_4pbpdc ligand displays one emission peak at 356 under excitation at 290 nm, while the emission peak of **InPCF-1a** is at 399 nm under the same excitation wavelength. The above emissions can be ascribed to the $\pi^* \rightarrow \pi$ or $\pi^* \rightarrow$ n transition of the ligand. Compared with free H_4pbpdc ligand, the obvious red-shift of 43 nm for **InPCF-1a** may be attributed to the $pbpdc^{4-}$ to In^{3+} charge transfer.[26] Besides, the organic ligand form strong π-π interactions with each other, which lower the energy of its excited state, leading to the observed red shift emission wavelength.

Owing to its good luminescence properties, thermal stability and the potential active site, **InPCF-1** has drawn our attention to use as luminescent probes in sensing metal ions. DMF was chosen as solute due to the poor dispersibility of **InPCF-1a** in water. The luminescent spectra of free H_4pbpdc ligand, **InPCF-1a** in DMF and **InPCF-1a** dispersed in DMF solution of different nitrate ($Co(NO_3)_2$, $Ni(NO_3)_2$, $Cu(NO_3)_2$, $Zn(NO_3)_2$) have been recorded. The emissions of free ligand and **InPCF-1a** in DMF are in good agreement with those in solid state (Fig. S12†). The luminescence intensities of **InPCF-1a-Cu^{2+}**, **InPCF-1a-Co^{2+}**, **InPCF-1a-Ni^{2+}**, and **InPCF-1a-Zn^{2+}** are largely dependent on the metal ions as shown in Fig. 5a. Decreases in the luminescence intensity could not be observed with the presence of Co^{2+}, Ni^{2+} and Zn^{2+}, while Cu^{2+} created a significant quenching effect on the system.

For comparison, we studied the influence of metal ions on the luminescence intensity of the free ligand. H_4pbpdc were dispersed in the same concentrations of Zn^{2+}, Co^{2+}, Ni^{2+} and Cu^{2+} in DMF solution. As demonstrated in Fig. 5b, except Zn^{2+}, Co^{2+}, Ni^{2+} and Cu^{2+} could generally induce the luminescence quenching at various degrees. The luminescence intensity of H_4pbpdc@DMF was enhanced by about 40 % with the addition of Zn^{2+}, indicating the potential of H_4pbpdc for the sensing of Zn^{2+}. However, **InPCF-1** instead of H_4pbpdc displays high selectivity toward Cu^{2+}. To examine the sensing sensitivity toward Cu^{2+} ions, a series of titration experiments were carried out. The emission responses were monitored by the gradual addition of different concentrations of $Cu(NO_3)_2$@DMF into the suspension of **InPCF-1a**@DMF. As illustrated on Fig. 5, the luminescence intensity at 399 nm gradually decreases as a function of increased the concentration of Cu^{2+}. The inset shows that

linear dependencies of luminescence intensities on the Cu^{2+} concentration were obtained. The limit of detection is down to 10^{-5} M, suggesting **InPCF-1** can be used for detecting trace Cu^{2+}. The quenching effect can also be quantitatively determined by the Stern-Volmer equation: $I_0/I=1 + K_{sv}[M]$. The values of I_0 and I are the luminescence intensities of **InPCF-1a**@DMF and metal-ion-incorporated **InPCF-1a**@DMF, respectively. [M] is the molar concentration of the metal ion, and K_{SV} is the quenching effect coefficient of the metal ion. The Stern-Volmer quenching coefficient (K_{sv}) for Cu^{2+} is calculated to be (1840.1 ± 45.9) M^{-1}, suggesting the high selectivity and sensitivity for Cu^{2+}. To the best of our knowledge, this value of quenching coefficient K_{sv}, 1840.1 M^{-1} for Cu^{2+} is the second highest in reported MOF materials (Table S3†).[8a,9] The result is comparable with those well designed organic compounds for sensing of Cu^{2+} (Typical K_{SV} is from 10^3 to 10^4 M^{-1}).[27] In addition, multiple cycles of Cu^{2+} sensing experiments have been performed and **InPCF-1a** could regain its intensity after filtration and washing by DMF (Fig. S13†).

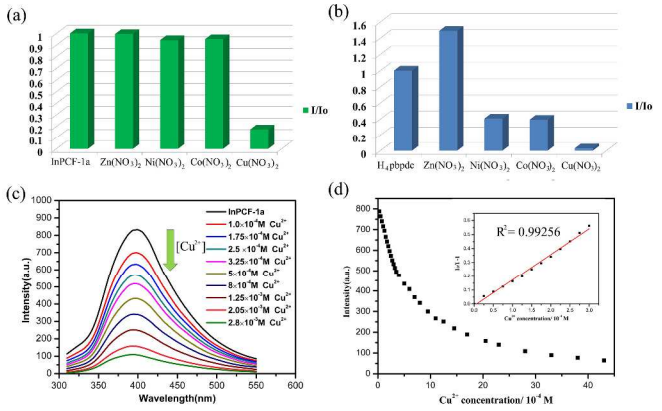

Fig. 5 (a)Comparison of the luminescence intensity of 399 nm of **InPCF-1a** incorporating 0.0028 M different metal ions DMF solution.(b) Comparison of the luminescence intensity of 356 nm of H_4pbpdc incorporating 0.0028 M different metal ions DMF solution. (c) and (d) Concentration-dependent luminescence intensities of **InPCF-1a** by the addition of different contents of copper nitrate DMF solution (Ex at 290 nm)

The framework integrities of metal-incorporation **InPCF-1a** samples were confirmed by PXRD patterns and the incorporation of Cu^{2+} can be easily observed by the naked eye (Fig. S14 and 15†) and Energy Dispersive X-ray spectra on **InPCF-1a-Cu^{2+}** indicated that the sample has a Cu: In ratio of 0.5 (Fig. S16†). We speculate that the recognition of Cu^{2+} ions might be related to the interaction between the Cu^{2+} ions and the uncoordinated carboxylate Lewis basic sites on **InPCF-1a**, similar to those reported MOFs.[8,9] The interaction between the Cu^{2+} ions and the pbpdc^{4-} ligands reduces the energy transfer efficiency from pbpdc^{4-} to the In^{3+} ions within **InPCF-1a**, thus decreasing the luminescent intensity. X-ray photoelectron spectroscopy (XPS) experiment on **InPCF-1a-Cu^{2+}** sample (Fig. S17†) showed that the typical energy of Cu 2p1/2 shifts to 955.2 eV, giving an increase of 3.0 eV compared with the standard value of free Cu^{2+}, indicating the interaction between Cu^{2+} ions and the materials. The Cu 2p3/2 peak at 935.2 eV is very close to the value of $Cu(OAc)_2$ (935.0 eV),[28] suggesting Cu^{2+} might interact with **InPCF-1a** by the pendent uncoordinated carbonyl groups inside the channel.

The highly selective and sensitive sensing of **InPCF-1** for Cu^{2+} ions inspired us to examine its application in sensing organic molecules. Due to devastating consequences on biological tissues, MV^{2+} was selected as the guest to study the sensing ability of **InPCF-1**. It is noteworthy that the intensity decreases to 50 % at the concentration of only 10^{-5} M MV^{2+}, allowing the sensor to detect the presence of even trace MV^{2+}. The increased amount of MV^{2+} resulted in a gradual decrease of luminescence intensity at 399 nm (Fig. S18†). Excellent linear dependencies of luminescence intensities on the MV^{2+} concentration were obtained. The Stern-Volmer quenching coefficient (K_{sv}) for MV^{2+} is calculated to be (23356.8 ± 451.7) M^{-1}, suggesting high sensitivity for MV^{2+}. Quenching phenomenon may be attributed to electrostatic interactions between cationic organic ions and anionic framework. This can be confirmed by the comparison test of biphenyl. The same concentration of biphenyl was added into **InPCF-1a** DMF, which turned out to have little influence on the luminescence of **InPCF-1a** (Fig. S19†).

Conclusions

In summary, a highly stable indium phosphonocarboxylate framework (**InPCF-1**) with functional sites was designed and synthesized. **InPCF-1** features rod-shaped SBU and 1-D straight channels. Its porosity was confirmed by CO_2 and liquid vapor adsorption. Importantly, it has the ability to selectivity sense Cu^{2+} ions due to interactions between Cu^{2+} and the functional sites inside the channel. **InPCF-1** also has high selectivity and sensitivity to MV^{2+}. These results could provide a facile route to design and synthesize novel metal phosphonate framework as promising multifunctional materials.

Acknowledgements

This work was financially supported by the National Natural Science Foundations of China (Nos. 21101031, 21171042 and 21203032), the Program for Changjiang Scholars and Innovative Research Team in University (IRT1117) and Shanghai Leading Academic Discipline Project (Project No. B108).

Notes and references

Department of Chemistry, Fudan University, 220 Handan Road, Shanghai 200433, P.R. China. Tel: +86-21-65643925, Fax: +86-21-65642261, e-mail:zhxchen@fudan.edu.cn; ymzhou@fudan.edu.cn

† Electronic Supplementary Information (ESI) available: Details of structural figures, TG result, PXRD patterns, adsorption data and Emission spectra. CCDC 1000500 contains the supplementary crystallographic data for this paper. See DOI: 10.1039/b000000x/

1. N. C. Burtch, H. Jasuja and K. S. Walton, *Chem. Rev.* **2014**, *114*, 10575–10612.

2. (a) K. Maeda, *Micropor. Mesopor. Mater.* **2004**, *73*, 47–55; (b) G. K. H., Shimizu, R. Vaidhyanathan and J. M. Taylor, *Chem. Soc. Rev.* **2009**, *38*, 1430–1449. (c) K. J. Gagnon, H. P. Perry, and A. Clearfield, *Chem. Rev.* **2012**, *112*, 1034–1054.
3. (a) T. B. Liao, Y. Ling, Z. X. Chen, Y. M. Zhou and L. H. Weng, *Chem. Commun.* **2010**, *46*, 1100–1102. (b) M. L. Deng, Y. Ling, B. Xia, Z. X. Chen, Y. M. Zhou, X. F. Liu, B. Yue and H. Y. He, *Chem. Eur. J.* **2011**, *17*, 10323–10328. (c) A. Dutta, M. Pramanik, A. K. Patra, M. Nandi, H. Uyamab, and A. Bhaumik, *Chem. Commun.* **2012**, 48, 6738–6740.
4. (a) Y. Ling, M. L.Deng, Z. X .Chen, B. Xia, X. F.Liu, Y. T. Yang, Y. M. Zhou and L. H. Weng, *Chem. Commun.* **2013**, *49*, 78–80. (b) F. P. Zhai, Q. S. Zheng, Z. X. Chen, Y. Ling, X. F. Liu, L. H. Weng and Y. M. Zhou, *CrystEngComm.* **2013**, *15*, 2040–2043.
5. F. P. Zhai, M. L. Deng, Y. Ling, Z. X. Chen and Y. M. Zhou, *Inorg. Chim. Acta* **2013**, *402*, 104–108.
6. J. M. Taylor, K. W. Dawson and G. K. H. Shimizu, *J. Am. Chem. Soc.* **2013**, *135*, 1193–1196.
7. (a) Y. Zhou, F. Wang, Y. S. J. Kim and J. Yoon, *Org. Lett.* **2009**, *11*, 4442–4445. (b) G. He, H. Peng, T. Liu, M. Yang, Y. Zhang and Y. Fang, *J. Mater. Chem.* **2009**, *19*, 7347–7353. (c) Z.Y. Guo, H. Xu, S. Q. Su, J. F. Cai, S. Dang, S. C. Xiang, G. D. Qian, H. J. Zhang, M. O'Keeffe and B. L. Chen, *Chem. Commun.*, **2011**, *47*, 5551–5553. (d) Y. Takashima, V. M. Martinez, S. Furukawa, M. Kondo, S. Shimomura, H. Uehara, M. Nakahama, K. Sugimoto and S. Kitagawa, *Nat. Commun.* **2011**, *2*, 168. (e) Y. Li, S. S. Zhang and D. T. Song, *Angew. Chem. Int. Ed.* **2013**, *52*, 710–713.
8. (a) B. L. Chen, L. B. Wang, Y. Q. Xiao, F. R. Fronczek, M. Xue, Y. J. Cui and G. D. Qian, *Angew. Chem. Int. Ed.* **2009**, *48*, 500–503. (b) J. Lan, K. H. Li, H. H. Wu, D. H. Olson, T. J. Emge, W. Ki, M. C. Hong, and Jing Li, *Angew. Chem. Int. Ed.* **2009**, *48*, 2334–2338. (c) Z. G. Xie, L. Q. Ma , K. E. deKrafft, A. Jin and W. B. Lin, *J. Am. Chem. Soc.*, **2010**, *132*, 922–923. (d) Z. Hao, X. Song, M. Zhu, X. Meng, S. Zhao, S. Su, W. Yang, S. Song and H. Zhang *J. Mater. Chem. A* **2013**, *1*, 11043–11050. (e) S. S. Nagarkar, B. Joarder, A. K. Chaudhari, S. Mukherjee, and S. K. Ghosh, *Angew. Chem. Int. Ed.* **2013**, *52*, 2881–2885. (f) L. Y. Pang, G. P. Yang, J. C. Jin, M. Kang, A. Y. Fu, Y. Y. Wang and Q. Z. Shi, *Cryst. Growth Des.* **2014**, *14*, 2954–2961.
9. (a) K. Jayaramulu, R. P. Narayanan, S. J. George and T. K. Maji, *Inorg. Chem.* **2012**, *51*, 10089–10091. (b) Y. Q. Xiao, Y. J. Cui, Q. Zheng, S. C. Xiang, G. D. Qian and B. L. Chen, *Chem. Commun.* **2010**, ***46***, 5503–5505. (c) J. M. Zhou, W. Shi, H. M. Li, H. Li and P. Cheng, *J. Phys. Chem. C* **2014**, *118*, 416–426. (d) B. Liu, W. P. Wu, L. Hou and Y.Y. Wang, *Chem. Commun.* **2014**, *50*, 8731–8734.
10. (a) Z. X. Chen, Y. M. Zhou, L. H. Weng, C. Yuan and D. Y. Zhao, *Chem. Asian J.* **2007**, *2*, 1549–1554. (b) Z. X. Chen, Y. M. Zhou, L. H. Weng and D. Y. Zhao, *Cryst. Growth Des.* **2008**, *8*, 4045–4053. (c) Z. X. Chen, Y. Ling, H. Y. Yang, Y. F. Guo, L. H. Weng and Y. M. Zhou, *CrystEngComm* **2011**, *13*, 3378–3382. (d) Z. X. Chen, H. Y. Yang, M. L. Deng, Y. Ling, L. H. Weng and Y. M. Zhou, *Dalton. Trans.* **2012**, *41*, 4079–4083. (e) M. L. Deng, X. F. Liu, Q. S. Zheng, Z. X. Chen, C. Y. Fang, B. Yue, H. Y. He, *CrystEngComm* **2013**, *15*, 7056–7061.
11. (a) T. Loiseau, C. Serre, C. Huguenard, G. Fink, F. Taulelle, M. Henry, T. Bataille and G .Férey, *Chem. Eur. J.* **2004**, *10*, 1373–1382. (b) M. Pang, A. J. Cairns, Y. Liu, Y. Belmabkhout, H. C. Zeng and M. Eddaoudi, *J. Am. Chem. Soc.* **2012**, *134*, 13176–13179. (c) F. Gándara, H. Furukawa, S. Lee and O. M. Yaghi, *J. Am. Chem. Soc.* **2014**, *136*, 5271–5274.
12. (a) S. T. Zheng, T. Wu, C. Chou, A. Fuhr, P. Y. Feng and X. H. Bu, *J. Am. Chem. Soc.* **2012**, *134*, 4517–4520. (b) S. T. Zheng, J. J. Bu, T. Wu, C. Chou, P. Y. Feng and X. H. Bu, *Angew. Chem. Int. Ed.* **2011**, *50*, 8858–8862. (c) S. T. Zheng, J. L. Bu, T. Wu, F. Zuo, P. Y. Feng and X. H. Bu, *J. Am. Chem. Soc.* **2010**, *132*, 17062–17064. (d) F. Nouar, J. Eckert, J. F. Eubank, P. Forster and M. Eddaoudi, *J. Am. Chem. Soc.* **2009**, *131*, 2864–2870. (e) Y. Liu, V. C. Kravtsov, D. A. Beauchamp, J. F. Eubank and M. Eddaoudi, *J. Am. Chem. Soc.* **2005**, *127*, 7266–7267. (f) F. Gándara, B. Gomez-Lor, E. Gutiérrez-Puebla, M. Iglesias, M. A. Monge, D. M. Proserpio, N. Snejko, *Chem. Mater.* **2008**, *20*, 72–76. (g) D. F. Sava, L. E. S. Rohwer, M. A. Rodriguez and T. M. Nenoff, *J. Am. Chem. Soc.* **2010**, *134*, 3983–3986.
13. Z. X. Chen, S. C. Xiang, T. B. Liao, Y. T. Yang, Y. S. Chen, Y. M. Zhou, D. Y. Zhao and B. L. Chen, *Cryst. Growth Des.* **2010**, *10*, 2775–2779.
14. W. Y. Dan, X. F. Liu, M. L. Deng, Z. X. Chen, Y. Ling and Y. M. Zhou, *Inorg. Chem. Commun.* **2013**, *37*, 93–96.
15. G.M. Sheldrick, *Acta Cryst.* **2008**, *A64*, 112–122.
16. R. A. Coxall, S. G. Harris, D. K. Henderson, S. Parsons, P. A. Tasker and R. E. P. Winpenny, *J. Chem. Soc. Dalton Trans.*, **2000**, 2349–2356.
17. S. S. Dhingra and R. C. Haushalter, *J. Chem. Soc. Chem. Commun.* **1993**, 1665–1667. (b) A. M. Chippindale, and S. J. Brech, *Chem. Commun*. **1996**, 2781–2782. (c) A. Thirumurugan, and S. Natarajan, *Dalton Trans*. **2003**, 3387–3391. (d) L. Wang, S. Shi, J. Ye, Q. Fang, Y. Fan, D. Li, J. N. Xu and T. Y. Song, *Inorg. Chem. Commun.* **2005**, *8*, 271–273; (e) L. Wang, T. Y. Song, J. N. Xu, Y. Wang, Z. Tian and S. Shi, *Micropor. Mesopor. Mater*. **2006**, *96*, 287–292. (f) Z. Dong, Y. Yan, Y. Li, J. Li, J. Yu and R. Xu, *Inorg. Chem. Commun.* **2011**, *14*, 727–730.
18. N. L. Rosi, J. Kim, M. Eddaoudi, B. Chen, M. O'Keeffe and O. M. Yaghi, *J. Am. Chem. Soc.* **2005**, *127*, 1504–1518.
19. A. L. Spek, PLATON, A Multipurpose Crystallographic Tool, Utrecht University, Utrecht, the Netherlands, 2002.
20. V. A. Blatov and A. P. Shevcenko, TOPOS version 4.0 Professional (beta evaluation), that is available at http://www.topos.ssu.samara.ru.
21. (a) Reticular Chemistry Structure Resource (RCSR), http://rcsr.anu.edu.au/. (b) J. F. Liu, F. P. Huang, H. D. Bian and Q. Z. Yu, *Anorg. Allg. Chem.* **2013**, *639*, 2347–2353. (c) L. P. Zhang, J. F. Ma, J. Yang, Y. Y. Pang and J. C. Ma, *Inorg. Chem.* **2010**, *49*, 1535–1550.
22. (a) S. S. Iremonger, J. Liang, R. Vaidhyanathan and G. K. H. Shimizu, *Chem. Commun.* **2011**, *47*, 4430–4432. (b) M. Taddei, F. Costantino, A. Ienco, A. Comotti, P. V. Dau and S. M. Cohen, *Chem. Commun.* **2013**, *49*, 1315–1317.
23. S. G. Kazarian, M. F. Vincent, F. V. Bright, C. L. Liotta and C. A. Eckert, *J. Am. Chem. Soc.* **1996**, *118*, 1729–1736.
24. K. Sumida, D. L. Rogow, J. A. Mason, T. M. McDonald, E. D. Bloch, Z. R. Herm, T. H. Bae and J. R. Long, *Chem. Rev.* **2012**, *112*, 724–781.

25. J. R. Li, R. J. Kuppler and H. C. Zhou, *Chem. Soc. Rev.* **2009**, *38*, 1477–1504.
26. (a) Z. Lin, L. Chen, C. Yue, C. Yan, F. Jiang, M. Hong, *Inorg. Chim. Acta* **2008**, *361*, 2821–2827. (b) Z. Guo, Y. Li, W. Yuan, X. Zhu, X. Li and R. Cao, *Eur. J. Inorg. Chem.* **2008**, 1326–1331.
27. (a) L. Jiao, J. Li, S. Zhang; C. Wei, E. Hao, M. Grac and H. Vicente, *New J. Chem.* **2009**, *33*, 1888–1893. (b) S. Goswami and R. Chakrabarty, *Tetrahedron Lett.* **2009**, *50*, 5910–5913.
28. NIST X-ray Photoelectron Spectroscopy Database, http://srdata.nist.gov/xps/

Graphical abstract

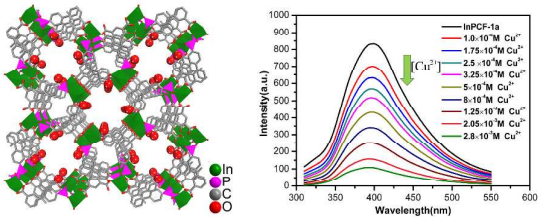

An indium phosphonocarboxylate framework (**InPCF-1**) with novel 3,4,5-connected topology was synthesized, which serves as selective and sensitive sensor for Cu^{2+} and MV^{2+} ions.